Pharmaceutical Research, Vol. 6, No. 6, 1989

Research Article

Permeability and Mechanism of Albumin, Cationized Albumin, and Glycosylated Albumin Transcellular Transport Across Monolayers of Cultured Bovine Brain Capillary Endothelial Cells

Kevin R. Smith[1] and Ronald T. Borchardt[1,2]

Received August 4, 1988; accepted January 31, 1989

We have measured the permeability and binding characteristics of bovine serum albumin (BSA), cationized BSA (cBSA), and glycosylated BSA (gBSA) to primary cultures of bovine brain capillary endothelial cells (BBCEC). These endothelial cells serve as an *in vitro* model to study the binding, uptake, and transcellular transport of small and large molecule flux across the blood–brain barrier. The rate of [^{3}H]BSA flux across the cultured BBCEC monolayers grown onto polycarbonate membranes (5-μm pore size) was linear with increasing BSA concentration and the flux could be inhibited by temperature reduction to 0–4°C. The maximal binding of [^{3}H]BSA was 0.04 fmol/mg total cell protein and could not be inhibited by nonradiolabeled BSA. The binding of cBSA and gBSA was rapid and could be inhibited by nonradiolabeled cBSA or gBSA, respectively. The maximal amount bound was 1.8 fmol/mg total cell protein for cBSA and 17.4 fmol/mg total cell protein for gBSA. The dissociation constants (K_d's) were 27 ± 13 and 3.7 ± 1.1 n*M* for cBSA and gBSA, respectively. The flux rates of cBSA and gBSA across the endothelial cell monolayers were linear with respect to concentration and they were approximately seven times greater than those observed for BSA. Each of the proteins appeared on the antiluminal side of the endothelial cell monolayers primarily (90%) as intact protein as determined by trichloroacetic acid (TCA) precipitations and sodium dodecyl sulfate (SDS)–polyacrylamide gel electrophoresis (PAGE). The results for BSA are similar to those observed for lucifer yellow, a fluid-phase endocytic marker. In contrast to BSA, the binding and transcellular transport of cBSA and gBSA appear to proceed by an adsorptive-phase endocytic mechanism.

KEY WORDS: blood–brain barrier; protein permeability; macromolecule transport; fluid-phase endocytosis; adsorptive endocytosis.

INTRODUCTION

The blood–brain barrier (BBB), which consists primarily of the endothelial cells that line the vasculature, restricts the flux of small polar molecules and macromolecules into and out of the brain. This restricted flux is caused by the tight intercellular junctions, the lack of membrane fenestrations, and the overall low pinocytotic activity of these cells, thus restricting intercellular and intracellular flux of proteins (1). An example of a macromolecule that exhibits limited permeability to the BBB is albumin, which constitutes 30% (w/w) of the plasma proteins and functions to maintain osmolality between the blood and the peripheral tissue.

Recently, Long and Holaday (2) showed that dexamethasone, a synthetic glucocorticoid used for the treatment of brain edema, could modulate the flux of ^{125}I-bovine serum albumin (BSA) in the brains of adrenalectomized rats. This effect of dexamethasone demonstrates the potential role of adrenal glucocorticoids in regulating the flux of proteins and possibly water across the BBB.

BSA is a large water-soluble protein with a molecular weight of 66,500. BSA is roughly a spherically shaped molecule having a hydrated radius of approximately 35 Å and a p*I* = 3.9. The physical chemical properties of BSA can be changed by glycosylation and cationization, which have been shown to influence the protein's vascular permeability *in vivo* and *in vitro* (1,3).

Earlier studies using intact microvessels isolated from rat epididymal fat showed that the vesicular ingestion rates for glycosylated (gBSA) and other carbohydrate modified albumins were approximately 1000 times greater than the rate observed for native albumin (3). These modified albumins also exhibit a higher affinity for mouse peritoneal macrophages (14). The nonenzymatic glycosylation of proteins, a process in which glucose is covalently bound to lysine groups on the protein due to long-term hyperglycemic conditions as found in diabetic patients, leads to clinical complications such as enzyme inactivation, basement membrane thickening, and hyperpermeable vessel walls (5).

When BSA is cationized, causing a change in the p*I*

[1] Department of Pharmaceutical Chemistry, School of Pharmacy, University of Kansas, Lawrence, Kansas 66045.

[2] To whom correspondence should be addressed.

0724-8741/89/0600-0466$06.00/0

from 3.9 to >9, the resulting cationized BSA (cBSA) exhibits enhanced binding to the brain microvessels (6) and exhibits increased flux into the cerebrospinal fluid of mice (7). cBSA coupled to β-endorphin binds to isolated bovine brain capillaries and was transported into the brain more rapidly than the uncoupled β-endorphin, thus providing a potential means for the delivery of nontransportable peptides to the brain (6).

Earlier our laboratory developed an *in vitro* BBB model system consisting of cultured bovine brain capillary endothelial cells (BBCEC) grown onto porous membranes (8). The goals of the research reported in this paper were to determine the nature of the interactions of BSA, cBSA, and gBSA with these cultured endothelial cells and to determine whether these proteins exhibit different permeabilities to the endothelial cells as has been reported *in vivo*. The results of these studies have provided valuable insight into how the physical chemical characteristics of a protein influence its ability to be endocytosed and transcytosed by fluid phase and adsorptive processes.

MATERIALS AND METHODS

Chemicals

[^{14}C]Sucrose (671 mCi/mmol) was purchased from DuPont NEN Chemicals (Boston, Mass.), [^{3}H]sodium borohydride ([^{3}H]$NaBH_4$; 20 mCi/mmol) was purchased from Amersham (Arlington Heights, Ill.), and [^{125}I]BSA (0.95 mCi/mg) and [^{125}I]Bolton-Hunter reagent (2165 Ci/mmol) were purchased from ICN Radiochemicals (Irvine, Calif.). Lucifer yellow CH was obtained from Molecular Probes, Inc. (Eugene, Ore.). Glycosylated albumin (albumin bovine glycosamide, 17–28 mol glucose/mol BSA) was purchased from Sigma Chemical Company (St. Louis, Mo.). All other chemicals were reagent grade or better.

Cationization of BSA

The isoelectric point (p*I*) of BSA was changed from an acidic p*I* 3.9 to a basic p*I* >9 by coupling ethylenediamine with carbodiimide to the BSA molecule using the method of Griffin and Giffels (7). Ethylenediamine (30.06 g) was dissolved in approximately 100 ml of distilled water and the pH was adjusted to 4.75 with 2 *N* NaOH, then brought to a final volume of 250 ml. Radioimmunoassay (RIA)-grade BSA (2 g) was dissolved in 4 ml of distilled water and added to the reaction mixture followed by the addition of 1-ethyl,-3-[3-dimethyl aminopropyl]carbodiimide hydrochloride (0.3625 g). The pH was maintained constant at 4.75. The reaction was quenched after 2 hr at 23°C by adding 1.3 ml of 4 *M* acetate buffer, pH 4.75. The resulting protein mixture was concentrated in an Amicon protein concentrator (Danvers, Mass., MW cutoff, 30,000) to 10 ml, then dialyzed overnight against 1 *M* NaCl. The cBSA was separated from BSA and further characterized by chromatofocusing using polybuffer exchanger 94 resin and polybuffer 96 elution buffer (Pharmacia Biotechnology Products, Piscataway, N.J.). The majority of the protein eluted in the void volume indicating the p*I* was >9. The cBSA was then lyophilized and stored at 4°C. The cBSA was also subjected to sodium dodecyl sulfate–polyacrylamide gel electrophoresis (SDS-PAGE) in 12% acrylamide using the Laemmli buffer system (9). The mobility of cBSA was similar to the mobility of native BSA.

Preparation of [^{3}H]BSA, [^{3}H]cBSA, and [^{3}H]gBSA

BSA, cBSA, and gBSA were tritiated by reductive methylation according to the method of Pardridge *et al.* (10). The protein (125 μg) was dissolved in 200 m*M* borate buffer, pH 8.9 (50 μl), and mixed with 10 μl of 0.4 *M* formaldehyde on ice followed by the addition of 1 mCi [^{3}H]$NaBH_4$ in a sealed glass reaction vial. After 10 min on ice, the mixture was removed by needle aspiration, applied to a 1 × 8-cm Sephadex G-25 column, and eluted with phosphate-buffered saline (PBS; 10 m*M* phosphate, 150 m*M* NaCl, pH 7.4). Fractions containing radioactivity and protein were pooled and dialyzed for 1 week at 4°C against fresh PBS. The resulting ^{3}H-labeled proteins were at least 97% trichloroacetic acid (TCA) precipitable. For specific activity measurements the protein content was assayed using a Bio-Rad protein assay kit and the radioactivity was measured by liquid scintillation spectroscopy.

Isolation and Culture of BBCECs

Microvessel endothelial cells were isolated from the cerebral gray matter of bovine brains as described by Audus and Borchardt (8). After isolation, approximately 3 × 10^6 cells were grown to confluence in 100-mm culture dishes. Prior to seeding, 5-μm-pore size polycarbonate filters (Nuclepore Co., Pleasanton, Calif.) were placed in the dishes and then they were coated with rat tail collagen and fibronectin and sterilized for 90 min in UV light. After 10–12 days in culture all filters were inspected by microscopy to determine the degree of confluency. The histochemical, biochemical, and morphological characteristics of the cells have been reported earlier (8), and the *in vitro* model system was shown to possess all the features of the BBB including tight intercellular junctions and the lack of membrane fenestrations, γ-glutamyl transpeptidase and alkaline phosphatase activities, and factor VIII antigen (11).

Binding of [^{3}H]BSA, [^{3}H]cBSA, and [^{3}H]gBSA to Cultured BBCECs

Binding studies were carried out using cell monolayers grown on collagen- and fibronectin-coated 35-mm culture dishes. Prior to conducting the protein binding studies the monolayers were washed two times with assay buffer (120 m*M* NaCl, 4.7 m*M* KCl, 1.3 m*M* $CaCl_2$, 1.2 m*M* $MgSO_4$, 25 m*M* NaH_2CO_3, 0.05 m*M* NaEDTA, 1.2 m*M* NaH_2PO_4, 10 m*M* Hepes, pH 7.4) and then incubated at 37°C for 15 min. The buffer was removed by aspiration and the monolayers were again washed two times followed by the addition of assay buffer containing 10 pmol of ^{3}H-labeled protein and varying amounts (0–3 μmol) of nonradioactive protein. [^{3}H]BSA was exposed to the cells for 2 hr (maximum incubation period prior to loss of cell viability), whereas [^{3}H]cBSA and [^{3}H]gBSA were exposed to the monolayers for 30 min to achieve maximal binding. All experiments were conducted at room temperature. At the end of the incubation period the cells were washed three times in fresh assay

buffer, after which the cells were removed from the dish by two, 1-ml aliquots of 0.2 *N* NaOH. The cell suspension was divided equally for radioactivity and total cell protein measurements (Bio-Rad protein assay).

Transcellular Transport of [^{3}H]BSA, [^{3}H]cBSA, and [^{3}H]gBSA Across Monolayers of BBCECs

Confluent monolayers of endothelial cells grown on polycarbonate membranes (13-mm diameter, 5-μm pore size) were placed in side-by-side diffusion cells with a 0.64-cm^2 diffusional area (Crown Glass Co., Somerville, N.J.) for protein flux measurements. The diffusion cells were maintained at a constant temperature (37 or 0–4°C) with a circulating water bath. The diffusion assay buffer (3.3 ml, 122 m*M* NaCl, 25 m*M* $NaHCO_3$, 10 m*M* D-glucose, 3 m*M* KCl, 1.2 m*M* $MgSO_4$, 0.4 m*M* $KHPO_4$, and 1.4 m*M* $CaCl_2$, pH 7.4) was added to both sides of the diffusion-cell apparatus.

In order to measure the time course of BSA flux, a pulse of [^{3}H]BSA (10–200 μl) was added to the donor side (the side exposed to the endothelial cells) of the diffusion apparatus and 50- to 200-μl aliquots were removed from both donor and receiver sides of the diffusion cells at specific time intervals. Each time point was corrected for dilution and instrumental background and then converted to nanomoles according to the measured specific activity of the protein. The diffusion assays were always carried out for 60 min, after which time the remaining buffer was removed and the cells were washed three times with 150 m*M* NaCl, 10 m*M* $NaHPO_4$, and 0.25% BSA, pH 7.4, for microscopic observation. In all cases the 60-min incubation did not alter the appearance of the cells. Samples containing [^{3}H]BSA were mixed with 10 ml of scintillation cocktail (3a70; Research Products International, Mt. Prospect, Ill.) and the radioactivity was measured with a Beckman Model LS6800 scintillation counter. The flux of [^{14}C]sucrose, a marker of extracellular flux, was measured in the same manner as described above. The fluxes of the [^{3}H]BSA and [^{14}C]sucrose were measured simultaneously, thus providing a means of measuring the integrity of the cell monolayer. The fluxes of [^{3}H]cBSA and [^{3}H]gBSA were measured by the same method as [^{3}H]BSA.

The permeabilities of [^{3}H]BSA, [^{3}H]cBSA, and [^{3}H]gBSA were determined by measuring the flux at various initial concentrations ranging from 0.01 to 3 μ*M*. The rates of protein flux were determined from the slopes of the linear regression. Each flux rate was normalized by the ratio of fractional [^{14}C]sucrose transport to fractional protein transport after 60 min. The flux of [^{14}C]sucrose served as an internal control for differences between cell monolayer integrity.

The normalized rates were then plotted against the corresponding initial concentration of transported compound for the determination of the permeability coefficients (*P*) according to Eq. (1):

$$P = kV/A \quad (1)$$

where *k* is the rate constant determined from the slope of the rate versus concentration plot times the assay volume (3.3 ml) and the ratio of cell volume to surface area (0.2 μm) was measured microscopically.

For comparison purposes the permeability of lucifer yellow (LY), a fluid-phase marker, was also measured across monolayers of bovine brain endothelial cells. The method for measuring the flux of LY was identical to the method for measuring ^{3}H-labeled protein flux except that the amount of LY crossing the monolayer was determined by measuring the increase in fluorescence in the receiver chamber. Fluorescence was determined by diluting an aliquot (200 μl) from the receiver side with 1 ml of deionized water. The fluorescence was measured using a SLM Model 4800 fluorescence spectrometer, with the excitation wavelength set at 430 nm and the emission wavelength set at 540 nm. Fluorescence calibration curves were constructed by serial dilution of LY each day before and after flux assay measurements. The detection limit for LY at these settings was <100 n*M*.

In order to determine if there was a significant loss of radiolabel or degradation of protein during transport across confluent monolayers of BBCEC in side-by-side diffusion cells, TCA precipitations and SDS-PAGE experiments were carried out. cBSA and gBSA were radioiodinated using Bolton-Hunter protein labeling kits according to the manufacturers specifications. The total donor concentration of protein was 5 mg/ml, which included approximately 3×10^6 cpm [^{125}I]BSA, [^{125}I]cBSA, or [^{125}I]gBSA. Samples of both donor and receiver chambers were subjected to SDS-PAGE [12% acrylamide, Laemmli buffer system (9)] after 1 hr of incubation at 37°C. The separated proteins were stained with Coomassie blue R-250 to visualize the protein bands, then each lane was cut into 1-cm pieces for counting with a Beckman model 5500 gamma counter. The TCA precipitability of the radioactive samples was also measured.

RESULTS

Binding of [^{3}H]BSA, [^{3}H]cBSA, and [^{3}H]gBSA to Cultured BBCECs

Binding studies to cell monolayers were conducted to determine the amount of specific and nonspecific binding of BSA, cBSA, and gBSA to the endothelial-cell monolayers. Figure 1A shows the femtomoles of total [^{3}H]BSA bound per milligram of total cell protein and the effect of varying the concentration of nonradiolabeled BSA on the binding of [^{3}H]BSA to the cells. The addition of nonradiolabeled BSA did not cause displacement of the bound [^{3}H]BSA. The maximum amount of [^{3}H]BSA bound to the cells was approximately 0.04 fmol/mg total cell protein. In contrast to [^{3}H]BSA, [^{3}H]cBSA and [^{3}H]gBSA showed a higher total binding (1.8 fmol/mg total cell protein for cBSA, 17.4 fmol/mg total cell protein for gBSA). The addition of excess nonradiolabeled cBSA displaces 0.3 fmol/mg total cell protein of the [^{3}H]cBSA as shown in Fig. 1B. Similarly the addition of an excess of nonradiolabeled gBSA displaced 13.6 fmol/mg total cell protein of the [^{3}H]gBSA in a saturable manner as shown in Fig. 1C. Dissociation constants (K_d's) and total and nonspecific binding values were calculated by fitting the following function to the displacement data (12):

$$B = B_o - (I * B_o)/(I + K_d) + NS \quad (2)$$

where *B* is the amount bound, B_o is the amount bound in the absence of competing substance (*I*), K_d is the dissociation

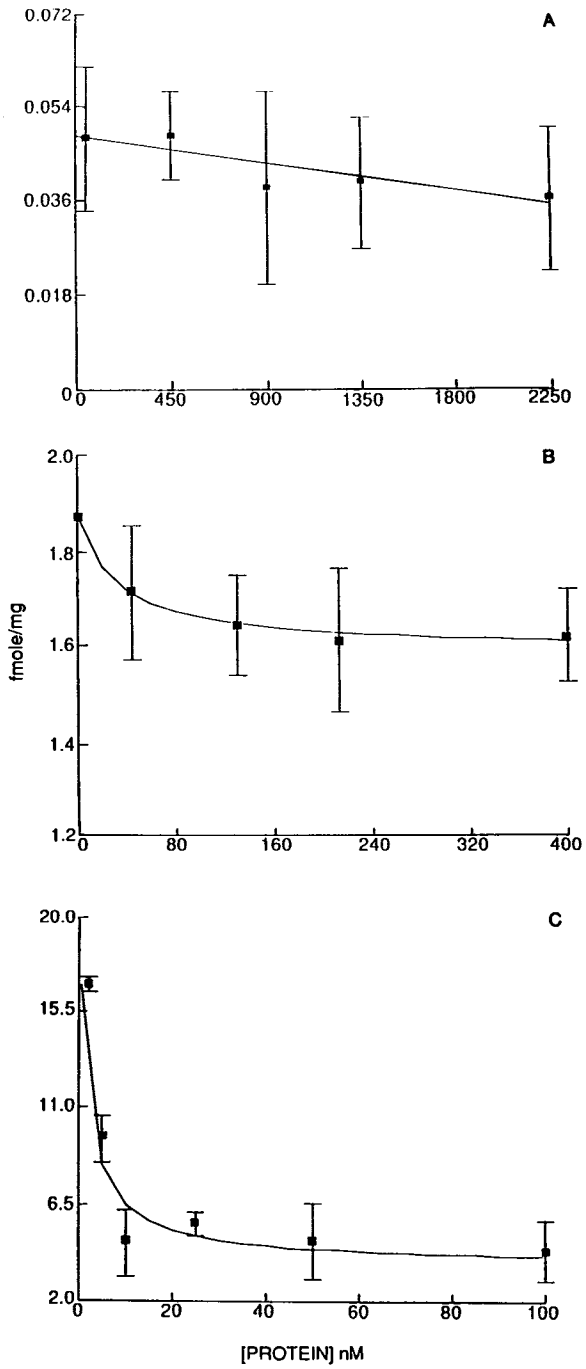

Fig. 1. Competitive displacement and binding of [^{3}H]BSA, [^{3}H]cBSA, and [^{3}H]gBSA to cultured monolayers of BBCECs. A shows the fraction of total [^{3}H]BSA bound to monolayers of BBCEC as a function of nonlabeled BSA from 0 to 2.2 μ*M* after 2 hr of incubation at 20°C. B is the displacement curve for [^{3}H]cBSA as a function of nonlabeled cBSA from 0 to 400 n*M*. The parameters from weighted nonlinear least-squares fitting of Eq. (2) to the data were B_o = 0.3 fmol/mg total cell protein, K_d = 27 ± 13 n*M*, and *NS* = 1.5 fmol/mg total cell protein. C is the data for [^{3}H]gBSA binding to BBCEC as a function of nonlabeled gBSA. The parameters from weighted nonlinear least squares fitting of Eq. (2) to the data were B_o = 13.6 fmol/mg total cell protein, K_d = 3.7 ± 1.1 n*M*, and *NS* = 3.8 fmol/mg total cell protein. All the data points represent the mean of three to five separate experiments ± SD. All binding was carried out at 20°C.

constant, and *NS* is the amount of nonspecific binding. The K_d's for cBSA and gBSA were 27 ± 13 and 3.7 ± 1.1 n*M*, respectively. All the parameters from the data analysis are summaried in Table I.

Transcellular Transport of [^{3}H]BSA, [^{3}H]cBSA, and [^{3}H]gBSA Across Monolayers of BBCECs

Figure 2 shows the concentration dependence of the flux rate of [^{3}H]BSA and [^{3}H]gBSA across monolayers of BBCECs. The flux rate of [^{3}H]BSA was very low and appears to be linear over the entire concentration range from 0 to ~1.5 μ*M*, which indicates passive diffusion across the cell layer. The flux rates of [^{3}H]gBSA (Fig. 2) and cBSA (data not shown) also show a linear increase with increasing concentrations of added protein over a concentration range of 0–2.5 μ*M*. It should be noted that the flux rate at any concentration of cBSA and gBSA was much greater then that for BSA. The higher flux rates of cBSA and gBSA are probably due to the binding of these proteins to the luminal surface of the cells prior to transcytosis. Also shown in Fig. 2 is the rate of flux of [^{3}H]BSA across only the collagen- and fibronectin-coated polycarbonate membrane. The results clearly show that the collagen- and fibronectin-coated filter was not the barrier to the flux of [^{3}H]BSA. Data for [^{3}H]cBSA and [^{3}H]gBSA (not shown) were exactly the same as the [^{3}H]BSA data. The possible degradation of the radiolabeled proteins during transport was measured by TCA precipitation and SDS-PAGE. At the end of the 1-hr incubation period, 90% of the proteins were TCA precipitable and migrated on SDS-PAGE to the same position as intact BSA, cBSA, and gBSA (data not shown), indicating an insignificant loss of radiolabel or degradation during transcellular transport.

Earlier Jacques (13) and Williams (14) proposed that the rate of adsorptive-phase endocytosis (adsorption to specific or nonspecific cellular binding sites followed by endocytosis) would saturate at low ligand concentrations followed by a linear increase in flux due to high-capacity fluid-phase endocytosis. In order to test this possibility the concentration–rate profiles for fluid phase and adsorptive phase endocytosis were simulated according to the expression suggested by Jacques (13):

$$R = SNC/(K + C) + FC \qquad (3)$$

where R is the overall rate of transport, S is the rate of surface uptake, F is the rate of fluid-phase uptake, N is the number of ligand binding sites, K is the dissociation constant of the ligand for the binding site, and C is the total concentration of the ligand. The first term in Eq. (3) represents the adsorptive component of the flux rate. When the receptors on the surface of the cell become saturated, the second component (FC) in Eq. (3) dominates the overall flux rate. In order to demonstrate the effect of a saturable or adsorptive component of the flux rate, we performed computer simulations of the apparent flux rate in the presence and absence of the fluid-phase component of the flux. The adsorptive-phase component alone saturates at approximately four times the dissociation constant used in the simulation, as shown in Fig. 3. When the fluid-phase component is added, the saturable portion of the curve assumes a rate equal to the rate of

Table I. Binding Parameters for ^{3}H-Labeled Proteins to Monolayers of Cultured BBCEC

Protein	K_d (nM)	fmol/mg		Index of specificity[a]
		Specific	Nonspecific	
BSA	∞	0.01	0.04	0.3
cBSA	27 ± 13	0.3	1.5	0.2
gBSA	3.7 ± 1.1	13.6	3.8	3.6

[a] fmol/mg total protein (specific)/fmol/mg total protein (nonspecific).

fluid-phase transcytosis, i.e., saturability is lost. The rate profile in the absence of binding was again linear and has a slope similar to the fluid-phase component for the total function, and the overall flux rate is lower at all concentrations. These findings indicate that saturation in the concentration dependence at low initial ligand concentrations was exaggerated and cannot be resolved from experimental or theoretical data. The function does not predict the observed increase in overall flux due to the concentrating effect of binding or alterations in intracellular trafficking events caused by surface adsorption.

Temperature Dependence of Molecular Flux Across Monolayers of BBCECs

In order to determine the mechanism responsible for the transcellular flux of [^{3}H]BSA, [^{3}H]cBSA, and [^{3}H]gBSA, we measured the flux of the fluid-phase marker, lucifer yellow (LY) (15), and the extracellular space marker, sucrose. The data in Fig. 4A show the concentration dependence of LY flux across monolayers of cultured endothelial cells. As expected for a fluid-phase marker, the flux of LY was concentration dependent and nonsaturable. Also shown in Fig. 4 is the effect of temperature on the flux of LY (A), [^{14}C]sucrose (B), and [^{3}H]BSA (C). The reduction in temperature from 37 to 0–4°C has a dramatic effect on the permeability of [^{3}H]BSA and LY. However, the effect of temperature on sucrose permeability was not as dramatic. The flux of [^{3}H]cBSA and [^{3}H]gBSA was completely inhibited at 0–4°C (data not shown) as is shown for [^{3}H]BSA and LY.

In order to verify further a cellular pathway of protein flux, the flux of the extracellular marker, sucrose, was measured with and without a cell monolayer at 37 and 0–4°C. The ratio of sucrose permeabilities at the two temperatures with and without cells was comparable to those predicted by the changes in diffusion coefficients calculated by the Stokes–Einstein relation,

$$D = kT/6\pi\eta rF \quad (4)$$

where D is the diffusion coefficient, k is Boltzman's constant, T is the absolute temperature, η is the solvent viscosity, r is the hydrated radius of the diffusing particle, and F is the particle shape factor. Assuming that the shape and radius of the particle do not change between 37 and 0°C, the ratio of diffusion constants reduces to a ratio of absolute temperatures and viscosities,

$$D_{37}/D_o = T_{37}\eta_o/T_o\eta_{37}, \quad (5)$$

where the subscripts refer to the temperatures in degrees centrigrade. The results for sucrose flux show that the effect was due only to the hydrodynamic properties of the solution, and not to the presence of a cell monolayer.

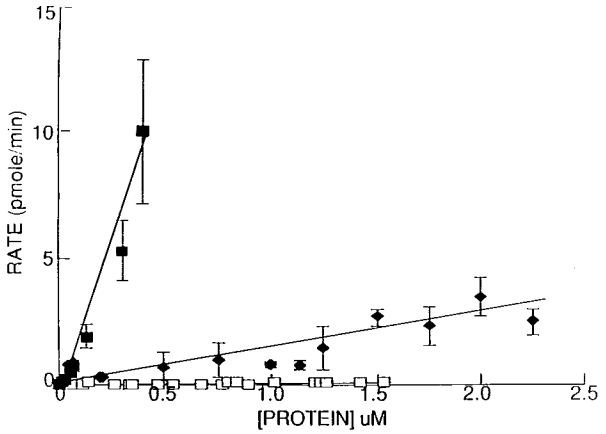

Fig. 2. Concentration dependence of [^{3}H]protein flux across collagen-coated polycarbonate filters with and without cultured monolayers of BBCECs. The rates of [^{3}H]BSA flux (□) and [^{3}H]gBSA (♦) are plotted against the indicated individual protein concentrations. Each data point was determined from the slope of the time course of protein flux. Also shown is the rate of [^{3}H]BSA flux (■) across collagen-coated polycarbonate filters (5-μm pore size). Each data point represents the mean of three to five experiments at a single concentration ± SD. All data were collected at 37°C.

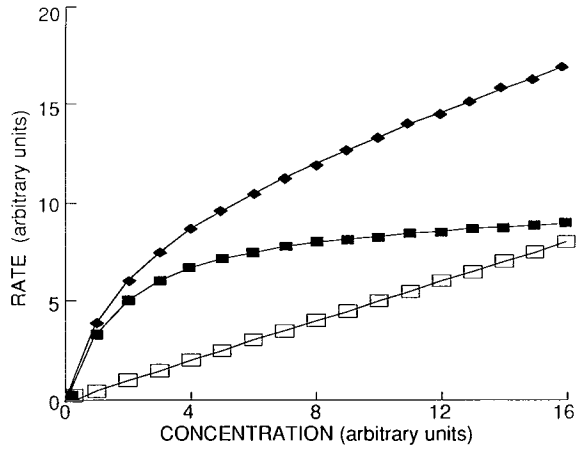

Fig. 3. Simulated concentration–rate profiles for fluid-phase and adsorptive-phase endocytosis. Concentration–rate profiles were simulated according to Eq. (3) in the text. Rate of flux for adsorptive-phase flux only (■): $F = 0$, $K = 2$, $S = 0.1$, $N = 100$. Rates of adsorptive- and fluid-phase flux (♦): $F = 0.5$, $K = 2$, $S = 0.1$, $N = 100$. Rate of fluid-phase flux only (□): $F = 0.5$, $K = 2$, $S = 0$, $N = 100$.

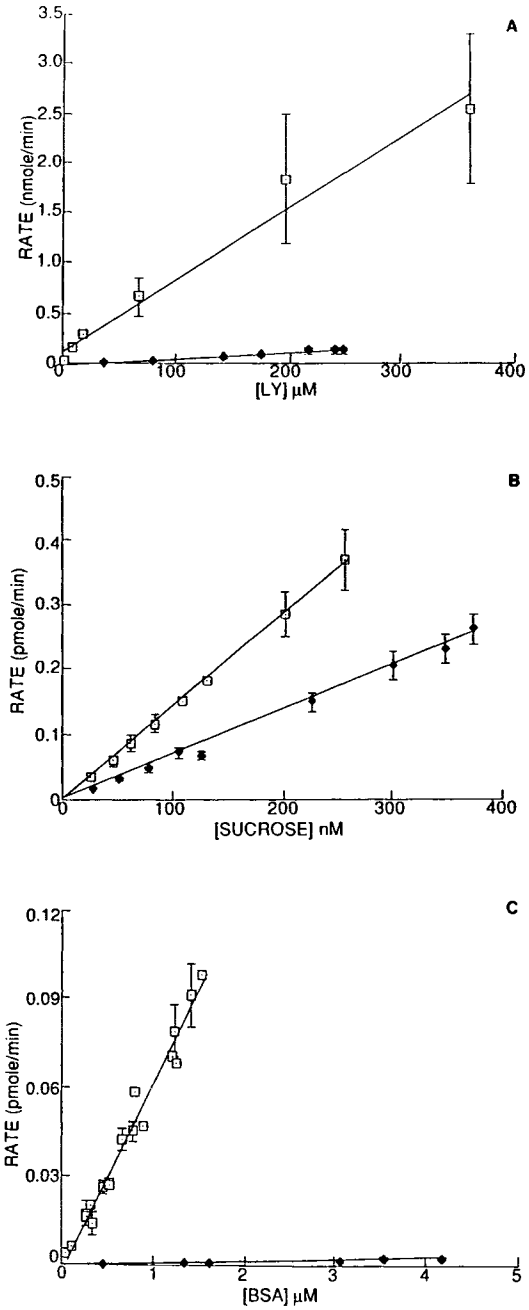

Fig. 4. Effect of temperature on the concentration dependence of LY, [^{14}C]sucrose, and [^{3}H]BSA flux rates across cultured monolayers of BBCECs. A shows the rate of LY flux at 37°C (□) and 0–4°C (♦), B shows the flux rate of [^{14}C]sucrose at 37°C (□) and 0–4°C (♦), and C shows the flux of [^{3}H]BSA at 37°C (□) and 0–4°C (♦). All data were obtained as described in the legend to Fig. 2 and represent the mean ± SD of three to five experiments.

Permeability Coefficients of [^{3}H]BSA, [^{3}H]cBSA, [^{3}H]gBSA, LY, and [^{14}C]Sucrose Across Monolayers of BBCECs

Table II summarizes the permeability coefficients for [^{3}H]BSA, [^{3}H]cBSA, [^{3}H]gBSA, LY, and [^{14}C]sucrose as well as comparative values from the literature for sucrose and BSA. The permeability coefficients were calculated from the slopes of the rate of flux vs concentration of diffusing substances as shown in Figs. 2 and 4. The permeability of the collagen-coated polycarbonate filter was accounted for by measuring the rate of flux in the absence of cells and the permeability coefficient was calculated as described above. The permeability coefficients of the cells alone (P_c) were determined by subtracting the inverse of the cell-free permeability coefficients (P_f's) from the inverse of the total permeability coefficients (P_t's) as described by Cooper *et al.* (16).

$$P_c = 1/(1/P_t - 1/P_f) \quad (6)$$

Table II. Permeability Coefficients for Transcellular Transport of Various Solutes Across Monolayers of Cultured BBCEC

Compound	P (cm · sec^{-1} × 10^{9})	
	Observed	Literature
BSA	0.85	29.[b]
cBSA	6.22	—
gBSA	6.71	—
LY	10.7	—
Sucrose	80.4	120.[c]

[a] Calculated from Eqs. (1) and (6).
[b] From ref. 16.
[c] From Ref. 21.

As shown in column 2 in Table II and in Fig. 2, cBSA and gBSA are 7.3 and 7.9 times more permeable than BSA to monolayers of cultured endothelial cells. Column 3 in Table II lists permeability coefficients from the literature for BSA flux in the dog heart capillary (17) and for sucrose flux in the rat brain (18). Comparison of the experimentally determined values to the literature values validates the methods used in this work and provides further evidence to support a cellular pathway of BSA transport since permeability coefficients for sucrose are comparable in the intact rat brain and in cultured BBCEC.

DISCUSSION

The mechanisms by which macromolecules and small polar molecules cross the brain capillary endothelial cells, which constitute the BBB, are important to elucidate in order to develop rational strategies for drug delivery to the brain. Until a suitable cell culture system of brain capillary endothelial cells was developed, BBB transport studies were conducted largely *in vivo*. While these *in vivo* experiments (18) shed considerable light on the properties of the BBB, the *in vitro* culture system, consisting of brain capillary endothelial cells (8) which were employed in this study, allows one to conduct controlled studies of many factors that can and do influence barrier permeability to drugs, nutrients, and macromolecules. The results described in this paper clearly demonstrate the utility of this culture system for elucidating the mechanism by which proteins undergo transcellular transport across the BBB.

The transcellular flux and the binding properties of BSA to cultured brain endothelial cells were consistent with a fluid-phase pinocytotic mechanism. The evidence for the mechanism of BSA flux came from the comparative studies with the flux of LY, a marker of fluid-phase endocytosis, and

the temperature dependence of the transcellular transport. The resulting data strongly favored BSA flux being similar to the flux of LY with respect to time, temperature, and concentration dependence. Specifically the concentration dependences of LY and the BSA fluxes were both linear and were highly temperature dependent. The lack of specific binding of the BSA to cell membranes also suggested a fluid-phase uptake mechanism. In addition to these results, BSA was insignificantly metabolized by the endothelial cells during transport. This conclusion was based on the determination of labeled protein (>90% TCA precipitable) in the receiver chamber of the diffusion cells.

The rates and temperature dependences of transcellular flux of LY and BSA observed in this study are consistent with the data reported by Guillot *et al.* (19) for the uptake of LY and horseradish peroxidase (HRP) using the identical cell culture system. Their data showed a low level of uptake and adsorption of these fluid-phase markers by the cultured endothelial cells.

Overall the permeability of the cultured endothelial cells to BSA was low as indicated by the calculated permeability coefficient (0.85×10^{-9} cm/sec). The permeability coefficient to cultured BBB endothelial-cell monolayers was approximately 34× lower than the permeability coefficient for BSA across nonfenestrated dog heart capillaries (17). The difference in BSA permeability coefficients between the dog heart capillaries and the bovine brain capillaries was no surprise since brain endothelial cells have tight intercellular junctions and low levels of pinocytotic activity, while heart capillaries do not.

Previously, Pardridge *et al.* (10) determined the relative permeability characteristics of the brain to BSA using the brain uptake index (BUI) method. They found the BUI of BSA to be similar to the uptake index for the extracellular space marker, sucrose. Based on these data, one might conclude that the permeabilities of sucrose and BSA were the same since the BUI method was not sensitive enough to measure small changes in permeability. However, our measurements using cultured BBCEC indicate that the permeability of BSA was, in fact, lower than the permeability for sucrose.

In contrast to BSA, cBSA and gBSA in part bind specifically to the endothelial cells (Fig. 1) and their apparent flux rates were much greater than the flux rate of BSA (Fig. 2). The other transport parameters were similar to that of BSA with respect to the linear concentration dependence, strong temperature dependence, and lack of degradation by the cells during transport. We believe that the enhanced flux rates of cBSA and gBSA result from the affinities that cBSA and gBSA exhibit for the endothelial cell and that their flux is mediated by adsorptive endocytosis.

The binding of cBSA probably occurs by nonspecific charge interactions as indicated by the large amount of nonspecific binding that was measured. Earlier studies by Kumagai *et al.* (6) with cBSA show that the positively charged protein binds rapidly and with a high affinity (K_d = 800 n*M*) to intact brain microvessels and that cBSA was displaced by polyamine and protamine sulfate (IC_{50} = 3 μg/ml), which indicates that a charge interaction between the cationized molecule and the anionic cell surface are major factors contributing to the overall binding of cBSA and that the binding was not specific for only cBSA. We report a much lower dissociation constant (28 n*M*) for cBSA to cultured bovine brain endothelial cells, which could be due to the presence of basement membrane in the intact microvessel preparation which has an affinity for cBSA (20).

Another factor that may contribute to the binding is a change in the conformation of the protein. It has been shown that cBSA greatly alters the immunogenic properties (20) of mouse T cells by increasing the number of antigenic determinates on the molecule which was evidence of structural alteration.

Binding of gBSA may be due to the affinity of the cell surface for glycosylated proteins (3,21), which produce rapid and high-affinity binding. The binding of gBSA to mouse peritoneal macrophages (5) was also reported to be rapid and showed a high affinity (K_d = 170 n*M*). Vlassara *et al.* (4) have suggested that there are specific receptors on the surface of the macrophage that are responsible for the removal of glycosylated proteins from the circulation. However, our data indicate that the binding of gBSA is not receptor mediated since the flux rate does not saturate but continues linearly even at very high protein concentrations as discussed above.

Adsorptive-phase pinocytosis involves the association or adsorption to specific and nonspecific receptors on the cell surface which may also enhance the internalization rate or alter intracellular trafficking events (22,23). Thus, the possible explanation for the higher transcellular flux rate for cBSA and gBSA versus BSA is that binding alters the percentage of ligand recycling to the external milieu, thus increasing the rate of transcytosis.

Guillot *et al.* (19) also studied the uptake and binding of adsorptive markers such as cationized ferritin and ricins by cultured BBCEC. The rate of uptake of these molecules, which show an affinity for the cultured endothelial cells, was enhanced as compared to fluid-phase markers and was consistent with the results we obtained for the transcellular flux in this study.

The measured permeability coefficients for cBSA and gBSA are approximately eight times greater than the permeability coefficients for BSA and are equivalent to the increase in BUI that was reported for cBSA (BUI = 11.8) (6) versus BSA (BUI = 0.98) (10).

Additional evidence in support of a pinocytotic mechanism of the flux of BSA, cBSA, and gBSA versus an intercellular pathway of transport came from the strong temperature dependence on the rate of flux of these proteins. The effect of temperature on pinocytosis is documented in the literature (14) and is clearly illustrated in our studies as shown in Fig. 4 for the flux of BSA, LY, and sucrose. There are two explanations for the large temperature dependence: (1) the inhibitory effect of low temperatures on chemical and biochemical reactions and (2) a lipid phase change that occurs between 10 and 15°C (24,25). The change from liquid crystalline to gel phase is likely to increase the rigidity of the lipid bilayer and, therefore, drastically reduce the amount of transcytosis.

Molecules known to penetrate the BBB have either the proper lipophilicity, molecular size, and shape (pore theory) to permit passive diffusion (26) or an affinity or a transport system present in the capillary endothelial cells. Overall, this

work demonstrates that methods of enhancing brain uptake should not be limited solely by size, charge, and lipophilicity but the possible interactions with specific or nonspecific receptors should be considered since cationic or glycosylated proteins such as cBSA and gBSA are large hydrophilic molecules which gain access to the brain through adsorptive transcytosis. In addition, this work illustrates the utility of our cell culture model of the BBB to probe and understand the factors that influence the permeability of the blood–brain barrier.

ACKNOWLEDGMENTS

This work was supported by a grant from The Upjohn Company, Kalamazoo, Mich. The authors gratefully acknowledge K. L. Audus and J. L. Wolfe for valuable discussions and critical reading of the manuscript.

REFERENCES

1. W. M. Pardridge. *Endocrine Rev.* 7:314–330 (1986).
2. J. B. Long and J. W. Holaday. *Science* 227:1580–1583 (1985).
3. S. K. Williams, J. J. Devenny, and M. W. Bitensky. *Proc. Natl. Acad. Sci. USA* 78:2393–2397 (1981).
4. H. Vlassara, M. Brownlee, and A. Cerami. *Clin. Chem.* 32:B37–B41 (1986).
5. M. Brownlee, H. Vlassara, and A. Cerami. *Ann. Intern. Med.* 101:527–537 (1984).
6. A. K. Kumagai, J. Eisenberg, and W. M. Pardridge. *J. Biol. Chem.* 262:15214–15219 (1987).
7. D. E. Griffin and J. Giffels. *J. Clin. Invest.* 70:289–295 (1982).
8. K. L. Audus and R. T. Borchardt. *Pharm. Res.* 3:81–87 (1986).
9. U. K. Laemmli. *Nature* 227:680 (1970).
10. W. M. Pardridge, J. Eisenberg, and W. T. Cefalu. *Am. J. Physiol.* 249:E264–E267 (1985).
11. A. Baranczyk-Kuzma, K. L. Audus, and R. T. Borchardt. *J. Neurochem.* 46:1956–1960 (1986).
12. R. C. Speth and S. I. Haricks. *Proc. Natl. Acad. Sci. USA* 82:6340–6343 (1985).
13. P. J. Jacques. In B. F. Trump and A. V. Arstila (eds.), *Pathobiology of Cell Membranes,* Academic Press, New York, 1975, pp. 255–282.
14. S. K. Williams. *N.Y. Acad. Sci.* 416:457–467 (1983).
15. J. A. Swanson, B. D. Yirinec, and S. C. Silverstein. *J. Cell Biol.* 100:851–859 (1985).
16. J. A. Cooper, P. J. Del Vecchio, F. L. Minnear, K. E. Burhop, W. M. Selig, J. G. N. Garcia, and A. B. Malik. *J. Appl. Physiol.* 63:1076–1083 (1987).
17. E. M. Renkin. *Acta Physiol. Scand. Suppl.* 463:81–91 (1979).
18. V. A. Levin. *J. Med. Chem.* 23:682–684 (1980).
19. F. L. Guillot, T. J. Raub, and K. L. Audus. *J. Cell Biol.* 105:312 (1987).
20. A. Muckerheide, R. J. Apple, A. J. Pesce, and J. G. Michael. *J. Immunol.* 138:833–837 (1987).
21. N. Shaklai, R. L. Garlick, and H. F. Bunn. *J. Biol. Chem.* 259:3812–3817 (1984).
22. J. L. Carpentier, P. Gorden, A. Robert, and L. Orci. *Experientia* 42:734–744 (1986).
23. K. S. Matlin. *J. Cell Biol.* 103:2565–2568 (1986).
24. B. R. Lentz, Y. Barenholz, and T. E. Thompson. *Biochemistry* 15:4521–4528 (1976).
25. B. R. Lentz, Y. Barenholz, and T. E. Thompson. *Biochemistry* 15:4529–4537 (1976).
26. J. D. Fenstermacher. *Trends Neurosci.* 8:449–453 (1985).